In-vivo Proton Magnetic Resonance Spectroscopy in Adnexal Lesions

Seong Whi Cho, MD[1, 2]
Soon Gu Cho, MD[1]
Jung Hee Lee, PhD[3]
Hyung-Jin Kim, MD[1]
Myung Kwan Lim, MD[1]
Jong Hwa Kim, MD[4]
Chang Hae Suh, MD[1]

Objective: To explore the *in-vivo* ^{1}H- MR spectral features of adnexal lesions and to characterize the spectral patterns of various pathologic entities.

Materials and Methods: Thirty-one patients with surgically and histopathologically confirmed adnexal lesions underwent short echo-time STEAM (stimulated echo acquisition method) ^{1}H- MR spectroscopy, and the results obtained were analysed.

Results: The methylene present in fatty acid chains gave rise to a lipid peak of 1.3 ppm in the ^{1}H- MR spectra of most malignant tumors and benign teratomas. This same peak was not observed, however, in the spectra of benign ovarian epithelial tumors: in a number of these, a peak of 5.2 ppm, due to the presence of the olefine group (-CH=CH-) was noted. The ratios of lipid peak at 1.3 ppm to water peak (lipid/water ratios) varied between disease groups, and in some benign teratomas was characteristically high.

Conclusion: An intense lipid peak at 1.3 ppm is observed in malignant ovarian tumors but not in benign epithelial tumors. ^{1}H- MRS may therefore be helpful in the differential diagnosis of adnexal lesions.

Index terms:
Magnetic resonance (MR), spectroscopy
Ovary, MR
Ovary, neoplasms

Korean J Radiol 2002;3:105-112
Received December 27, 2001; accepted after revision March 11, 2002.

[1]Department of Radiology, Inha University College of Medicine; [2]Department of Radiology, Hallym University College of Medicine, Hangang Sacred Heart Hospital; [3]NMR Laboratory, Asan Institute for Life Sciences; [4]Department of Obstetrics and Gynecology, Inha University College of Medicine

This study was supported by Inha University Research Grant INHA-21074 and was presented and exhibited at RSNA 2000.

Address reprint requests to:
Chang Hae Suh, MD, Department of Radiology, Inha University College of Medicine, 7-206 3rd St., Shinheung-dong, Choong-gu, Incheon 400-103, South Korea.
Telephone: (8232) 890-3401
Fax: (8232) 890-2743
e-mail: suhchae@inha.ac.kr

Most adnexal lesions manifest as cystic masses and differential diagnosis on the basis of imaging findings is difficult. Ultrasonography with color Doppler is currently the standard imaging tool for the differential diagnosis of adnexal masses, and although very sensitive in detecting these and sometimes able to indicate malignancy, it is frequently unable to provide images adequate for specific diagnosis. Physical examinations and the CA 125 serum level are helpful in some cases, and CT and MR imaging are increasingly used to evaluate pelvic masses; malignancy can in some cases be predicted, but since tumors can be graded and histologically assessed to only a limited extent, the results are no better than those obtained with ultrasonography (1-6).

Localized *in-vivo* proton magnetic resonance spectroscopy (^{1}H- MRS) has been shown to provide information about the contents of organic compounds in living tissues, providing details of tumor metabolism that might well assist tumor grading and lead to a better understanding of the biochemical pathways found within a lesion (7-14). As for ovarian tumors, however, the use of ^{1}H- MRS has -because of technical difficulty- been limited to *in-vitro* studies such as the analysis of aspirated fluid samples (11). The *in-vitro* ^{1}H- MR spectrum shows significantly different metabolite concentrations between benign and malignant ovarian cysts: in the latter, significantly higher levels of lactate, isoleucine, valine, 3-hydroxybutylic acid, methionine, and alanine are detected. The recent use of short echo-time (TE) ^{1}H- MRS has facilitated the observation of macromolecules and lipids, in addition to small molecules. For lipids to give rise

to a resonance peak that is narrow enough to be detectable by *in-vivo* ^{1}H- MRS, their fatty acyl chains must have a significant degree of mobility, and such lipids are therefore described as "mobile" (12). In tumors of the brain and uterine cervix, an elevated lipid peak, as demonstrated by ^{1}H- MRS, is thought to be a possible indicator of malignancy (12, 13): in ^{1}H- MR spectra of these tumors, the presence of the methylene group, CH_3, at 1.3 ppm, and the olefine group, -CH=CH-, at 5.2 ppm, is observed in those that are malignant.

In adnexal lesions, the acquisition of a good quality *in-vivo* ^{1}H- MR spectrum is very difficult because of motion artifacts caused by respiratory and bowel movements. Moreover, ^{1}H- MR spectroscopy using STEAM with short echo-time might be a more difficult and complex process due to its lower signal-to-noise ratio (SNR) during data acquisition and post-processing. The purpose of this study is to explore the *in-vivo* ^{1}H- MR spectral features of adnexal lesions using short echo-time and to characterize the spectral patterns of various pathologic entities.

MATERIALS AND METHODS

Patients

Thirty-one patients aged 22-69 (mean ±SD, 40 ±14) years with surgically proven adnexal lesions were included in this study. There were seven primary or secondary malignant ovarian tumors (2 papillary serous cystadenocarcinomas, 1 mucinous cystadenocarcinoma, 1 sarcomatoid carcinoma, and 3 metastatic adenocarcinomas), one borderline malignant mucinous cystic tumor, six benign epithelial tumors (3 mucinous cystadenomas, 1 serous cystadenoma, 1 serous cystadenofibroma, and 1 benign mixed epithelial tumor), eleven benign teratomas, four endometrioses, one ectopic pregnancy, and one case of salpingitis (Table 1). The maximal diameter of the lesions ranged from 4 to 23 cm, which in all cases was greater than the localization voxel for ^{1}H- MRS. Prior to ^{1}H- MRS,

Table 1. *In-vivo* ^{1}H-MR Spectroscopic and Pathologic Findings of Adnexal Lesions

Patient No.	Age(y)	^{1}H-MR Spectroscopic Findings			Histopathologic Diagnosis
		Peak at 1.3 ppm	Peak at 5.2 ppm	Lipid/Water Ratio	
1	54	Yes	No	0.007	Papillary serous cystadenocarcinoma
2	61	Yes	No	0.009	Papillary serous cystadenocarcinoma
3	50	Yes	No	NA	Mucinous cystadenocarcinoma
4	61	No	No	NA	Sarcomatoid carcinoma
5	62	Yes	No	0.006	Metastatic adenocarcinoma
6	48	Yes	No	0.007	Metastatic adenocarcinoma
7	45	No	No	NA	Metastatic adenocarcinoma
8	29	Yes	No	0.006	Borderline malignant mucinous cystic tumor
9	57	No	No	0.011	Mucinous cystadenoma
10	52	No	No	NA	Mucinous cystadenoma
11	28	No	No	NA	Mucinous cystadenoma
12	45	No	No	0.005	Serous cystadenoma
13	25	No	No	0.006	Serous cystadenofibroma
14	25	No	No	0.007	Benign mixed epithelial tumor
15	42	Yes	No	0.013	Teratoma
16	37	Yes	No	0.341	Teratoma
17	29	Yes	No	0.005	Mature cystic teratoma
18	39	Yes	No	0.061	Mature cystic teratoma
19	22	Yes	No	0.071	Mature cystic teratoma
20	31	Yes	No	0.273	Mature cystic teratoma
21	23	Yes	No	0.319	Mature cystic teratoma
22	36	No	Yes	0.005	Mature cystic teratoma
23	52	No	Yes	0.008	Mature cystic teratoma
24	25	No	No	0.004	Mature cystic teratoma
25	36	No	No	0.007	Mature cystic teratoma
26	25	No	Yes	0.006	Endometriosis
27	40	No	Yes	0.007	Endometriosis
28	30	No	No	0.004	Endometriosis
29	24	No	No	0.006	Endometriosis
30	69	Yes	No	0.010	Acute and chronic salpingitis with necrosis
31	44	No	Yes	0.010	Ectopic Pregnancy

Note.— NA= not available

pelvic CT and/or MRI was performed in all patients, none of whom has undergone treatment or biopsy.

MR Spectroscopy

For *in-vivo* ^{1}H- MRS, a 1.5-T whole-body GE MRI/MRS system (Signa Horizon; General Electric Medical Systems, Milwaukee, Wis., U.S.A.) equipped with active shielded gradients was used. Prior to ^{1}H- MRS, pelvic CT or MRI findings were reviewed by a radiologist to determine the location of adnexal lesions. MR imaging using a fast multiplanar spoiled gradient-echo (FMPSPGR) sequence (TR/TE= 100/1.5, NEX=1, matrix size=256 ×128, slice thickness=8.0 mm, interslice gap=2.0 mm) was performed in which the localization voxel was placed on the adnexal lesion. Voxel size was approximately 8 cm^3 (2 ×2 ×2cm), and the voxel was located safely within the lesion in order to reduce contamination from adjacent normal tissue. For all spectra, a STEAM (stimulated echo acquisition method) localization sequence combined with a three-pulse CHESS (chemical shift selective sequence) to suppress the H_2O signal was used, and the acquisition parameters were as follows: TR=3000 ms, TE=30 ms, number of scans=128, and number of excitations=1. During spectroscopic signal acquisition, the subjects respired quietly without interruption. Respiratory gating was not used in this study.

Spectral Analysis and Statistical Methods

Post-processing involving the use of a SUN SPARC 20 workstation with Spectral Analysis/General Electric (SA/GE) software; incorporated in this were low-frequency filtering of residual water signal, apodization by 0.5 Hz of exponential line broadening, zerofilling of 8000, Fourier transformation, and lorenzian-to-gaussian transformation.

^{1}H- MR spectra both with and without water-peak suppression were obtained, and all spectra were analysed with particular attention to the presence of lipid peaks at 1.3 and 5.2 ppm, and a water peak at 4.77 ppm. Lipid/water ratios were calculated by integrating the peak area of the

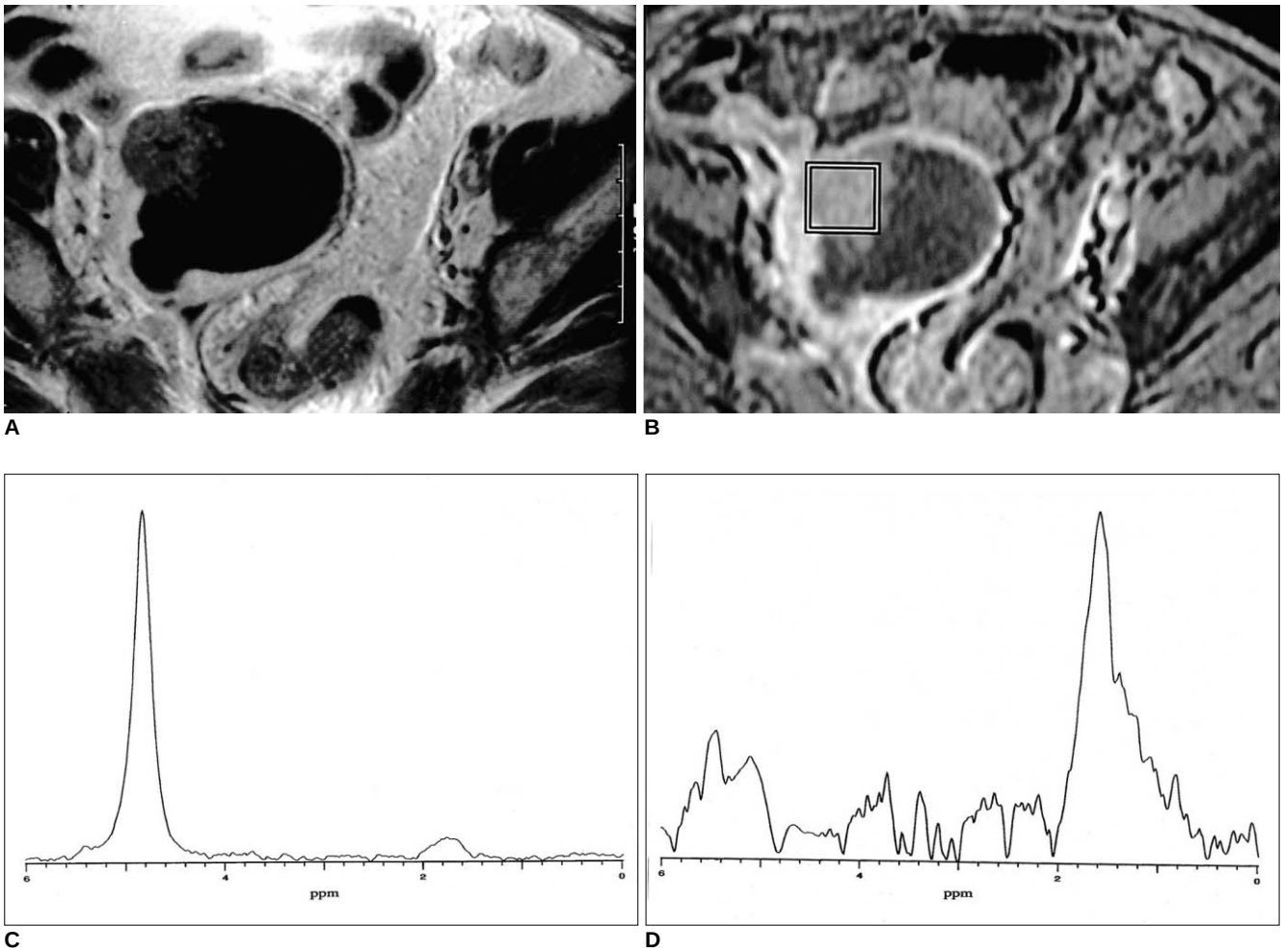

Fig. 1. Patient 2. Mucinous cystadenocarcinoma in a 61-year old woman. (**A**) Gadolinium-enhanced axial MR image and (**B**) axial scanogram obtained using ^{1}H- MRS reveal a cystic tumor with a solid nodular component. A prominent lipid peak occurred at about 1.3 ppm in (**C**) water-unsuppressed and (**D**) water-suppressed spectra, and the calculated lipid-to-water ratio was 0.009.

lipid peak at 1.3 ppm and water peaks in water-unsuppressed spectra. In spectra that demonstrated a dominant lipid peak at about 1.3 ppm, the highest peak point ±0.3 ppm of both the lipid and water peak was integrated. In ^{1}H- MR spectra that showed no dominant lipid peak, a range of 1.0-1.6 ppm was integrated in order to determine lipid content. The chi-square test was used to analyse spectroscopic data, and difference rankings between means at a statistically significant level were thus established. A p value of 0.05 was considered statistically significant.

RESULTS

A resonance peak at 1.3 ppm, caused by the presence of the methylene group in fatty acid chains, was observed in five of the seven malignant ovarian tumors and seven of the eleven benign teratomas (Figs. 1, 4), as well as in one borderline malignant tumor and the case of salpingitis (Fig. 2). Interestingly, whereas most primary and secondary malignant ovarian tumors showed an intense lipid peak at 1.3 ppm, this same peak was not observed in the MR spectra of any of the six benign ovarian epithelial tumors (Fig. 3). Thus, the incidence of a lipid peak was significantly higher in malignant tumors than in benign epithelial tumors ($p < 0.05$). A lipid peak at 5.2 ppm, due to the presence of the olefine group in fatty acid chains, was observed in two cases of the eleven benign teratomas, one of the four endometrioses, and the ectopic pregnancy. The ^{1}H- MR spectra of benign ovarian epithelial tumors showed no detectable lipid peak at 1.3 or 5.2 ppm (Tables 1, 2).

The lipid/water ratio was determined in 26 cases and was smaller than 0.020 in 21 of these. The lipid/water ratios of benign teratomas showed great variation, and some were higher than those of other adnexal lesions. In addition, all five cases in which the lipid/water ratio was greater than 0.020 were benign teratomas ($p < 0.05$).

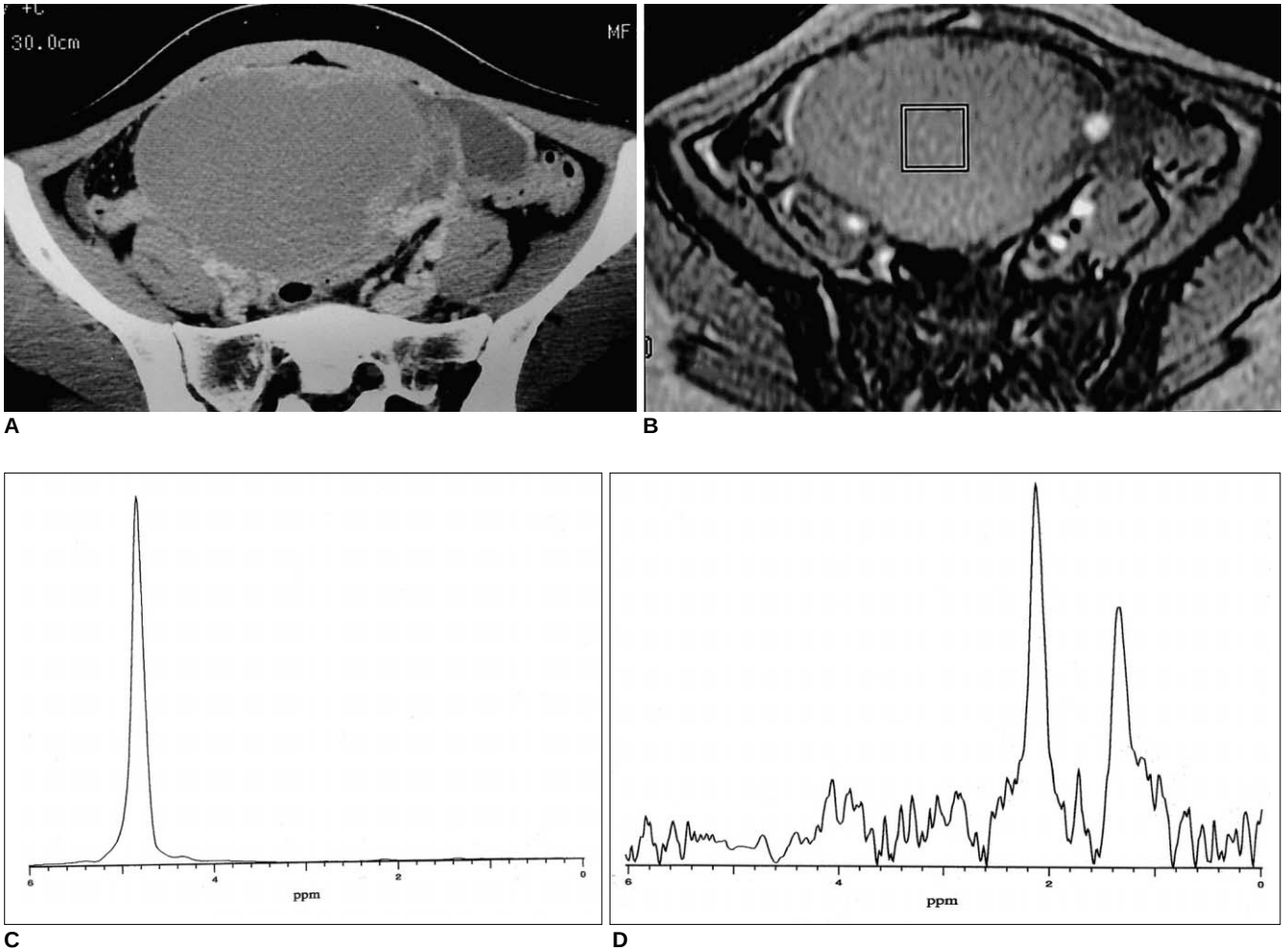

Fig. 2. Patient 8. Borderline malignant mucinous cystic tumor in a 29-year-old woman. (**A**) Pelvic post-contrast CT scan and (**B**) axial scanogram obtained using ^{1}H- MRS show a large multiseptated cystic mass with nodular enhancing peripheral portions. A prominent lipid peak was noted at 1.3 ppm in (**C**) water-unsuppressed and (**D**) water-suppressed spectra, and the lipid-to-water ratio was 0.006.

DISCUSSION

In our study, ^{1}H- MR spectroscopic patterns differed markedly according to the histopathologic diagnosis of the adnexal lesions. In fatty acid chains, the presence of the methylene group caused a resonance peak at 1.3 ppm in most patients with malignant ovarian tumors, benign teratomas and salpingitis. However, no lipid peak at 1.3 ppm was found in the ^{1}H- MR spectra of benign ovarian epithelial tumors or endometrioses.

In many previous studies involving *in-vivo* and *ex-vivo* MRS of brain tumors and uterine cervical carcinomas, the resonance peak due to fatty acid chains has been suggested as a possible cancer marker (12-14); the results of our study also support this possibility. Interestingly, Gotsis et al. (14) reported that ^{1}H- MRS demonstrated the presence of lipids in malignant brain tumors, abscesses and epidermoid cysts, but not in benign brain tumors. They assumed that necrosis and lipid formation might be the result of tumor proliferation without a neovascular network sufficient for its metabolic needs. Kuesel et al. (12) used *ex-vivo*

Table 2. Comparison of Peaks and Lipid/Water Ratios in MR Spectroscopy of Various Ovarian Lesions

Histopathologic Diagnosis	No. of Cases Showing Peaks at MRS		Lipid/ Water Ratio
	Lipid peak at 1.3 ppm	Lipid peak at 5.2 ppm	
Malignant tumor	5/7*	0/7	0.007 ± 0.001†
Borderline malignant tumor	1/1	0/1	0.006
Benign epithelial tumor	0/6*	0/6	0.007 ± 0.002†
Endometriosis	0/4	1/4	0.006 ± 0.001†
Benign teratoma	7/11*	2/11	0.101 ± 0.138†
Salpingitis	1/1	0/1	0.010
Ectopic pregnancy	0/1	1/1	0.010

Note.— *statistical significance ($p < 0.05$), as determined by the chi-square test; †mean ± 1 standard deviation

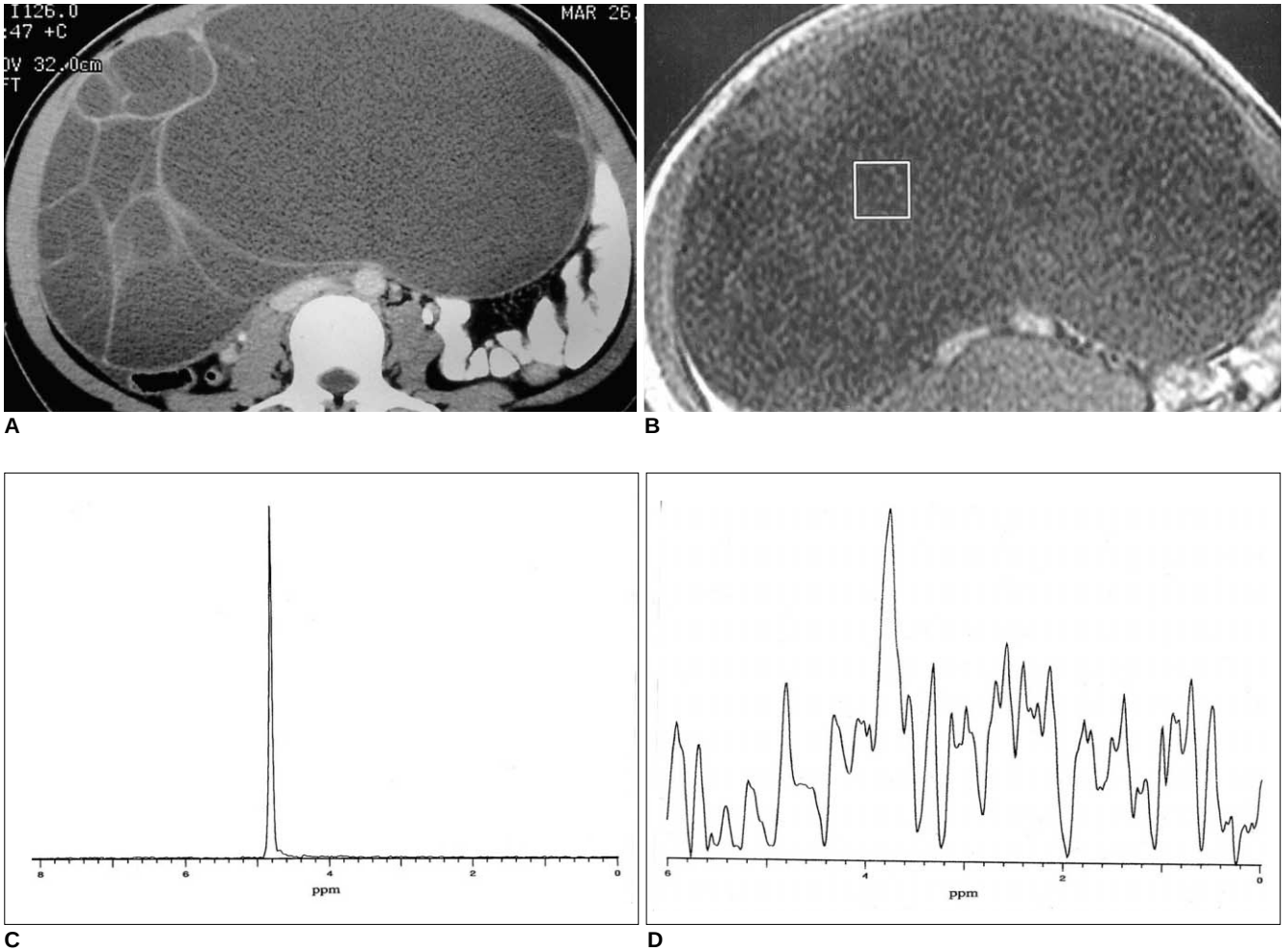

A **B** **C** **D**

Fig. 3. Patient 11. Mucinous cystadenoma in a 28-year-old woman. (**A**) Post-contrast CT scan and (**B**) axial scanogram obtained using ^{1}H- MRS demonstrate a large multiseptated cystic pelvic mass. There was no prominent lipid peak at 1.3 ppm in either (**C**) water-unsuppressed or (**D**) water-suppressed spectra, and the lipid-to-water ratio was unavailable.

^{1}H- MRS to evaluate mobile lipid resonance at biopsy or in surgical specimens of cerebral astrocytomas, discovering that in high-grade tumors, ^{1}H- MRS is able to detect high lipid levels. Rapid cellular turnover in malignant tissue usually leads to considerable cellular death, resulting in cellular necrosis, which appears in *in-vivo* ^{1}H- MR spectra as a lipid signal. This was previously observed in a study of human cervical carcinoma using *in-vivo* ^{1}H- MRS; invasive cervical carcinoma could be differentiated from normal cervix by a peak at 1.3 ppm, with 89% sensitivity and 57% specificity (13). In our study, a ^{1}H- MR spectral peak at 1.3 ppm was detected in malignant or borderline malignant ovarian tumors, with 75% sensitivity (6/8) and 65% specificity (15/23).

Because the T2 values of fatty acids and macromolecules are very short, ^{1}H- MRS using a short TE is required for the detection of these molecules. Owing to overlap in the spectral peaks demonstrated by macromolecules and lipids, the peaks obtained with short TE values (< 40 msec) are not as well resolved as those obtained with TE values greater than 90 msec (15-17). To avoid overlap between a lipid peak and one due to other metabolites at 1.3 ppm, the peak at 5.3 ppm caused by the presence of olefine has sometimes been used to identify the lipid component of a tumor (12). However, it can be assumed that because the baseline of the spectrum is relatively flat, the peaks occurring at about 1.3 ppm in the short TE MR spectrum of the human ovary are due mainly to the presence in fatty acid chains of the methylene group, and possibly lactate, but not macromolecules. According to a report by Massuger et al. (11), *in-vitro* ^{1}H- NMR studies of ovarian cystic fluids have disclosed that the amount of metabolites such as lactate, methionine, pyruvic acid, and 3-hydroxybutylic acid found in malignant cysts was over six times greater than in

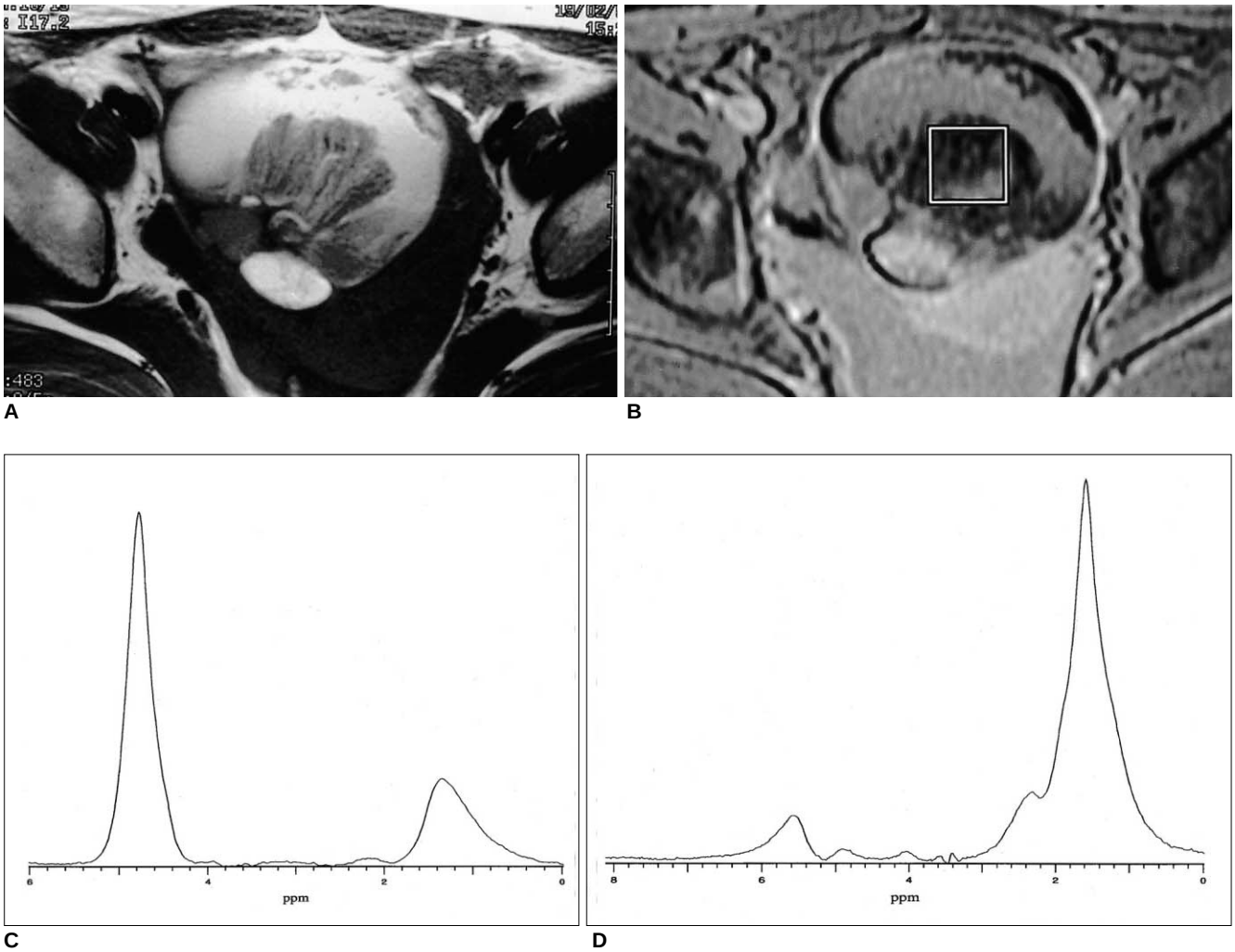

Fig. 4. Patient 21. Benign mature cystic teratoma in a 23-year-old woman. (**A**) Transaxial T1-weighted (TR/TE=483/9) image and (**B**) axial scanogram obtained using ^{1}H- MRS show a large pelvic mass with a heterogeneous internal texture. The focal, bright, high signal intensity of the tumor indicates its fat component. A very prominent lipid peak at about 1.3 ppm in (**C**) water-unsuppressed and (**D**) water-suppressed spectra was apparent, and the lipid-to-water ratio was 0.319.

benign cysts. In our study, however, the only MR spectral difference between benign and malignant ovarian tumors was the lipid peak at 1.3 ppm. Numerous metabolites, including amino acids, fatty acids, and other small molecules are found in ovarian cysts, but due to their limited concentration (i.e. sensitivity) and intrinsic properties such as T1 and T2 relaxation times, *in-vivo* ^{1}H- MRS was able to detect only a limited variety. Thus, in our study, we assumed that the peaks occurring at 1.3 ppm were due mainly to a tumor's lipid component. Evidence which also supported our assumption was the occurrence of a prominent peak at 1.3 ppm in most benign mature cystic teratomas in our study.

The combination of long- and short-TE spectra may be useful for evaluating the presence within a tumor of metabolites, lipids, and macromolecules (18). In studies of brain and uterine cervical tumors, ^{1}H- MRS using long TE has been used to detect long-T2 lipid components: nonmalignant cells of normal lipid have a short T2 value and are thus apparent only in the spectrum of short TE. Lipid components in a malignant tumor, on the other hand, assumed to have a long T2 (> 400 msec), can be detected by long-TE ^{1}H- MRS (13, 14, 19). The lipid peak thus detected is therefore attributed to malignant ovarian tissues with long T2 values, and this may indeed imply that the ^{1}H-MR spectroscopic technique is sensitive to early cellular change. In the case of pelvic MRS examination, signal intensity is influenced by motion artifact caused by respiratory and peristaltic bowel movement; an NMR study reported that the high susceptibility of the volume localization sequence to motion was a major disadvantage of short-TE STEAM ^{1}H-MRS (20). Hence we used both short- and long-TE MRS at the beginning of this study, but found that the waveforms of long-TE MR spectra were very irregular and non-informative, probably due to artifact. Long- and short-TE MRS data could not be combined, and only short-TE MR spectra could be analysed.

Only a few studies using ^{1}H- MRS have tried to differentiate between ovarian tumors and other pelvic lesions (11, 13, 21). In order to avoid the broad disturbing spectral resonances caused by protein protons, Massuger et al. (11) recently analysed *in-vitro* ^{1}H- NMR data of deproteinized ovarian cyst fluid samples. The *in-vitro* ^{1}H- NMR spectra obtained showed significant differences in metabolite concentrations between benign and malignant ovarian cysts, and significantly higher levels of lactate, isoleucine, valine, 3-hydroxybutylic acid, methionine and alanine were detected in malignant epithelial ovarian cysts. According to them, the elevated metabolite level and branched-chain amino acids found in malignant ovarian tumors most likely result from anaerobic glycolysis and enhanced proteolysis. In our study, however, these peaks were not usually detected by *in-vivo* ^{1}H- MR spectroscopy because the minimal concentration detectable by 1.5-T MR instruments is currently tens of millimoles.

Although various lesions in our study demonstrated a lipid peak at 1.3 ppm, the lipid/water ratio was useful to differentiate ovarian lesions. As they can be diagnosed easily by the detection of a lipid component at CT or MRI, teratomas demonstrated characteristically greater lipid/water ratios than other ovarian lesions; all our five cases in which the lipid/water ratio was greater than 0.020 were teratomas.

This study has several limitations, one of which is that ^{1}H- MR spectroscopic and radiologic findings were not compared. Another is the small number of cases studied. In order to establish indications of *in-vivo* ^{1}H- MR spectroscopic diagnosis, further investigation involving a large number of cases is required.

In conclusion, various ovarian lesions can be distinguished by careful disclosure of *in-vivo* ^{1}H- MR spectra, and *in-vivo* ^{1}H- MRS is potentially able to discriminate between malignant and benign tumors. The presence of a lipid peak at 1.3 ppm is a useful indicator of malignancy.

References

1. Granberg S, Norstrom A, Wikland M. Tumors in the lower pelvis as imaged by vaginal sonography. *Gynecol Oncol* 1990; 37:224-229
2. Levine D, Feldstein VA, Babcook CJ, Filly RA. Sonography of ovarian masses: poor sensitivity of resistive index for identifying malignant lesions. *AJR* 1994;162:1355-1359
3. Carlson KJ, Skates SJ, Singer DE. Screening for ovarian cancer. *Ann Intern Med* 1994;121:124-132
4. Buist MR, Golding RP, Burger CW, et al. Comparative evaluation of diagnostic methods in ovarian carcinoma, with emphasis on CT and MRI. *Gynecol Oncol* 1994;52:191-198
5. Stevens SK, Hricak H, Stern JL. Ovarian lesions: detection and characterization with Gadolinium-enhanced MR imaging at 1.5 T. *Radiology* 1991;181:481-488
6. Hermann UJ, Locher GW, Goldhirsch A. Sonographic patterns of ovarian tumors: prediction of malignancy. *Obstet Gynecol* 1987;69:777-781
7. Choi C-G, Lee HK, Yoon J-H. Localized proton MR spectroscopic detection of nonketotic hyperglycemia in an infant. *Korean J Radiol* 2001;2:239-242
8. Chang K-H, Kim HD, Park S-W, et al. Usefulness of single voxel proton MR spectroscopy in the evaluation of hippocampal sclerosis. *Korean J Radiol* 2000;1:25-32
9. Kim SH, Chang K-H, Song IC, et al. Brain abscess and brain tumors: discrimination with *in-vivo* H-1 MR spectroscopy. *Radiology* 1997;204:239-245
10. Lim MK, Suh CH, Kim HJ, et al. Systemic lupus erythematosus: brain MR imaging and single-voxel hydrogen 1 MR spectroscopy. *Radiology* 2000;217:43-49
11. Massuger LF, van Vierzen PB, Engelke U, Heerschap A, Wevers R. ^{1}H-magnetic resonance spectroscopy: a new technique to dis-

criminate benign from malignant ovarian tumors. *Cancer* 1998;82(9):1726-1730
12. Kuesel AC, Briere KM, Halliday WC, Sutherland GR, Donnelly SM, Smith ICP. Mobile lipid accumulation in necrotic tissue of high-grade astrocytomas. *Anticancer Research* 1996;16:1485-1490
13. Lee JH, Cho KS, Kim Y-M, et al. Localized *in-vivo* ^{1}H nuclear MR spectroscopy for evaluation of human uterine cervical carcinoma. *AJR* 1998; 170:1279-1282
14. Gotsis ED, Fountas K, Kapsalaki E, Toulas P, Peristeris G, Papadakis N. *In-vivo* proton MR spectroscopy: the diagnostic possibilities of lipid resonances in brain tumors. *Anticancer Research* 1996;16:1565-1568
15. Behar KL, Rothman DL, Spencer DD, Petroff OAC. Analysis of macromolecule resonances in ^{1}H NMR spectra of human brain. *Magn Reson Med* 1994;32:294-302
16. Hwang J-H, Graham GD, Behar KL, Alger JR, Prichard JW, Rothman DL. Short echo time proton magnetic resonance spectroscopic imaging of macromolecule and metabolic signal intensities in the human brain. *Magn Reson Med* 1996;35:633-639
17. Posse S, Schuknecht B, Smith ME, van Zijl PCM, Herschkovitz N, Moonen CTW. Short echo time proton MR spectroscopic imaging. *J Comput Assist Tomogr* 1994;17:1-14
18. Hwang J-H, Egnaczyk GF, Ballard E, Dunn RS, Holland SK, Ball WS Jr. Proton MR spectroscopic characteristics of pediatric pilocytic astrocytomas. *AJNR* 1998;19:535-540
19. Mountfold CE, Saunders JK, May GL, et al. Classification of human tumors by high-resolution magnetic resonance spectroscopy. *Lancet* 1986;1:651-652
20. Moonen CTW, von Kienlin M, van Ziji PCM, et al. Comparison of single shot localization methos (STEAM and PRESS) for *in-vivo* proton NMR spectroscopy. *NMR Biomed* 1989;2:201-208
21. Schiebler ML, Miyamoto KK, White M, Maygargen SJ, Mohler JL. In vitro high resolution ^{1}H-spectroscopy of the human prostate: benign prostatic hyperplasia, normal peripheral zone and adenocarcinoma. *Magn Reson Med* 1993;29:285-291